scientific reports

Check for updates

OPEN

Host brain environmental influences on transplanted medial ganglionic eminence progenitors

Rosalia Paterno ✉, Thy Vu, Caroline Hsieh & Scott C. Baraban

Interneuron progenitor transplantation can ameliorate disease symptoms in a variety of neurological disorders. The strategy is based on transplantation of embryonic medial ganglionic eminence (MGE) progenitors. Elucidating how host brain environment influences the integration of interneuron progenitors is critical for optimizing this strategy across different disease states. Here, we systematically evaluated the influence of age and brain region on survival, migration, and differentiation of transplant-derived cells. We find that early postnatal MGE transplantation yields superior survival and more extensive migratory capabilities compared to transplantation during the juvenile or adult stages. MGE progenitors migrate more widely in the cortex compared to the hippocampus. Maturation to interneuron subtypes is regulated by age and brain region. MGE progenitors transplanted into the dentate gyrus sub-region of the early postnatal hippocampus can differentiate into astrocytes. Our results suggest that the host brain environment critically regulates survival, spatial distribution, and maturation of MGE-derived interneurons following transplantation. These findings inform and enable optimal conditions for interneuron transplant therapies.

Cell transplantation is a promising therapy for neurological diseases as it provides an opportunity to modify neuronal networks. Debilitating conditions, such as epilepsy, neuropsychiatric disorders, Alzheimer's disease, or schizophrenia are characterized by alterations in inhibitory synaptic transmission linked to loss of subpopulations of GABAergic interneurons[1–5]. These pathologies, collectively referred to as "inter-neuropathies"[6], profoundly alter neuronal networks, contributing to the generation of abnormal brain activity. Neurostimulation approaches, such as deep brain stimulation (DBS) or responsive neurostimulation (RNS), provide a degree of control by directly stimulating inhibitory pathways within dysfunctional brain networks[7,8]. These approaches require the intracranial placement of electrodes in targeted brain regions, but do not provide selective activation of inhibition, as local excitatory neurons are also stimulated. A cell transplantation strategy capable of introducing subsets of inhibitory interneurons to selectively modify GABAergic circuits, in specific brain regions implicated in these diseases, offers a more targeted network-based option. However, to be effective, a cell transplantation therapy should satisfy some critical conditions: (i) adequate cell survival in the host brain following transplantation, (ii) effective migration in targeted host brain regions, (iii) differentiation into specified interneuron subtypes, and (iv) functional integration into existing neuronal networks. Embryonic medial ganglionic eminence (MGE) progenitor cells appear to satisfy these criteria[9]. Indeed, embryonic MGE cell transplantation has shown promising results in preclinical models representing several of these neurological diseases[10–13].

The overall premise for using embryonic MGE progenitors for cell transplantation was initially established by Wichterle and colleagues[14]. Using MGE progenitors from mouse embryos, they demonstrated that these cells give rise to GABAergic interneurons following transplantation into the cortex of host pups at postnatal day 2 (P2). MGE is a transient embryonic structure defined anatomically and by its unique transcription factor profile[15,16]. Progenitor cells from this sub-pallial proliferative zone migrate tangentially in streams to populate the neocortex, hippocampus, and striatum. Upon reaching these brain regions, MGE progenitors differentiate into two major GABAergic interneuron sub-classes: (1) parvalbumin-expressing (PV) fast-spiking interneurons, including basket and chandelier cells, and (2) somatostatin-expressing (SST) interneurons, mostly represented by Martinotti cells[17]. Similar to normal development, transplanted MGE progenitors exhibit robust migratory and differentiation capabilities[18]. Moreover, from a network perspective, MGE-derived interneurons functionally integrate into the host brain, where they receive synaptic input from endogenous neurons, make appropriate layer-specific synaptic connections onto endogenous excitatory neurons[19,20], and enhance GABA-mediated inhibition[21] in a

Department of Neurological Surgery and Weill Institute of Neuroscience, University of California, 513 Parnassus Ave, Health Science East, E840, San Francisco, CA 94143, USA. ✉email: rosalia.paterno@gmail.com

subtype specific manner, i.e., PV-positive MGE-derived neurons innervate cell somas, and SST-positive MGE-derived interneurons innervate dendritic regions.

Despite the success of embryonic MGE progenitor transplantation for ameliorating disease symptoms in animal models of Alzheimer's disease[11,13], Parkinson's disease[22], epilepsy[10,23], neuropathic pain[24], traumatic brain injury (TBI)[12], schizophrenia[25], and autism[26], the optimization of this approach for specific brain regions and developmental stages has not been addressed. Although not directly explored in prior studies, as yet unknown aspects of the host brain environment are likely to be critical to effective transplantation and integration of MGE-derived interneurons for such a wide variety of neurological disorders. One notable issue among prior adaptations of MGE transplantation is the reported variability of MGE-derived cell survival which ranges from 1 to 20%[18,27,28]. A second issue is the number of injections necessary to obtain adequate migration of cells across the targeted brain region, with some publications reporting cell concentrations as high as 200,000 cells per injection and others only 15,000 per site[21,29]. A third issue is the developmental stage of the recipient animal, as limited migration and parvalbumin-positive cell differentiation were observed in some adult transplants. Taken together, these issues suggest that host brain environment is a critical determinant in the survival, migration and differentiation of MGE-derived interneurons following transplantation.

Here, we address these issues to better understand environmental factors and conditions influencing the effective integration of embryonic MGE progenitors following transplantation. Embryonic MGE progenitors were transplanted during different developmental stages (pup, juvenile, and adult) and into different brain regions critical to Alzheimer's disease, epilepsy, TBI, schizophrenia and autism (cortex and hippocampus). Sacrificing recipient animals at 30 days after transplantation (DAT), we carefully assessed survival, migration, and maturation profiles. Micro-targeting of MGE cell transplantation to specific hippocampal sub-regions was also explored in an effort to potentially tailor this strategy for more focal manipulation of neuronal circuitry. Early postnatal transplantation yielded better MGE-derived cell survival rates and more extensive migratory capabilities compared to transplantation into juvenile and adult brains. The host brain region also influenced these factors, with the cortex showing a greater capacity to receive MGE-derived interneurons than the hippocampus. Within the hippocampus, transplanted MGE progenitors showed unique migration and differentiation fates depending on the hippocampal sub-region where MGE progenitor cells were initially deposited. Altogether, this information highlights age- and region-specific environmental factors that influence successful implementation of embryonic MGE progenitor cell transplantation as a potential therapy for neurological diseases.

Material and methods

Animals

All experiments were performed on mice maintained on a 12-hour light/12-hour dark cycle with no food or water restrictions. All procedures involving animals followed the guidelines of the National Institutes of Health and were approved by Institutional Animal Care and Use Committee at University of California, San Francisco (#AN181254-02B). Embryonic donor tissue was obtained by crossing wild-type CD1 mice (Charles River Laboratories, Cat Num #022) with homozygous beta-actin EGFP mice on a CD1 background. We used male and female CD1 and male C57BL/6J (Jackson laboratory; 000664) mice as recipients. The study was conducted in accordance with the ARRIVE (Animal Research: Reporting of in Vivo Experiments) guidelines.

Tissue dissection and transplantation

MGE progenitor cells were harvested from E13.5 GFP+ transgenic embryos, as previously described[10,13]. In brief, embryonic day 0.5 was defined when the vaginal plug was detected. To dissect MGE, embryonic brains were first removed, the telencephalon isolated and the two hemispheres separated by a sagittal cut. The ventral telencephalon was exposed, and the medial ganglionic eminence was isolated using the sulcus that clearly divide the medial from lateral ganglionic eminence. The dorsal MGE was collected after removing the preoptic area and mantle zone. MGE progenitor cells were collected in Leibovitz L-15 media, mechanically dissociated in a single-cell suspension in media containing DNase I (Roche, 100 ug/ml) using repeated pipetting, and concentrated by centrifugation (3 min at 800×*g*). Cells were kept at 4 °C until transplantation.

Concentrated GFP+ MGE cells (~600 cells per nl) were injected using 30° beveled glass micropipettes (80 µm diameter tip, Witerol 5 µl, Drummond Scientific) prefilled with mineral oil into the cortex or hippocampus of recipient pup (P2–4), juvenile (P30–40) and adult (P90–150) animals. Pipettes were attached to a microinjector (Narishige) mounted on a stereotaxic machine (Kopf). We quantified cell viability of MGE cells using Triptan Blue (Sigma), and a viability more than 80% was considered as cutoff to proceed with transplantation. Each cortical recipient animal received a single injection containing 5×10^4 cells. Hippocampal recipient animals received a single or a double injection per hemisphere containing 3×10^4 cells due to an increased risk of clumping when using higher volumes.

Pups were anesthetized by exposure to ice until pedal reflexes were absent. Around 50–100 nl of highly concentrated cells were injected at the following coordinates from bregma to target the cortex (1.2 mm anterior, 1.2 mm lateral, and 0.6 mm dorsal) or the hippocampus (1.2 mm anterior, 1.2 mm lateral, and 1.4 mm dorsal). After injection, pups were returned to their mothers. Juvenile and adult animals were anesthetized by a mixture of ketamine/xylazine. Cell injections were made into the cortex at the following coordinates from bregma: anterior–posterior (AP) – 1.75 mm, medial lateral (ML) 1.75 mm, and dorsal-ventral (DV) 0.6 mm. For the hippocampus, injections to target the stratum radiatum of area CA3 or the stratum oriens of area CA1 were made at the following coordinates: AP – 2 mm, ML 2.5 mm, DV 1.8 mm and AP – 2 mm, ML 1.6 mm, DV 1.15 mm, respectively.

Immunohistochemistry

Mice were deeply anesthetized with a mixture of Ketamine/Xylazine and perfused transcardially with saline, followed by 4% paraformaldehyde (PFA; Electron Microscopy Science). Brains were post-fixed with PFA 4% overnight, and 50 µm thick coronal sections were cut with a VT 1000S vibratome (Leica Microsystems Inc., Buffalo Grove, IL). Free-floating vibratome sections were processed as follows. Sections were washed in PBS and blocked for 1 h in PBS containing 10% goat serum at room temperature. Sections were then incubated overnight in primary antibodies at 4 °C, washed in PBS and incubated with secondary antibodies for 2 h at room temperature in the dark. Primary antibodies used included anti-NeuN (Millipore; MAB377; 1:500), anti-GFP (AvesLabs; GFP-1020; 1:1000), anti-parvalbumin (Sigma-Aldrich; P3088; 1:1000), anti-somatostatin (Santa Cruz Biotech, SC55565, 1:200), anti-GABA (Sigma, A2052, 1:500), anti-GFAP (Millipore, MAB3402, 1:500), anti-Oligo2 (Millipore, AB9610, 1:300), and anti-CC1 (Sigma-Aldrich; OP80; 1:500). Secondary antibodies used were Alexa 488 (Invitrogen; A11039; 1:1000), Alexa 594 (Invitrogen; A11005; 1:1000), and Alexa 647 (Invitrogen; A21244; 1:1000).

Cell counts and quantification

Images were acquired at 1024 pixels resolution using a Nikon confocal microscope. Quantification analysis was performed with NIS-Elements software (Nikon) on fluorescently labeled sections (50 µm) captured with 4×, 10×, and 40× objectives. All transplanted cells expressing GFP were counted in every sixth coronal section (spaced 300 µm apart) across all layers of the cortex or hippocampus, as previously described[21]. To estimate cell survival in each hemisphere, we counted the number of GFP+ cells in every 6-coronal section (spaced 300 µm apart) along the rostro-caudal axis. This count was multiplied by 6, and the survival rate was calculated as (total survived cells/numbers of transplanted cells) *100. To assess the distribution of GFP+ cells across cortical layers, GFP+ cells were assigned to one of 10 bins superimposed on the area between pial surface (bin 1) and white matter (bin 10). To determine the percentage of grafted GFP+ cells co-expressing NeuN, SST, PV, GFAP, Oligo or CC1 after transplantation (n = 3 mice per marker), we quantified the number of GFP+ cells co-expressing these antibody markers in every sixth coronal section (spaced 300 µm apart).

Statistical analysis

All analyses were performed using PRISM (GraphPad). Two-tailed t-tests, unpaired t-tests and one-way ANOVA's were employed as specified in each analysis to compare different groups. All plots with error bars are reported as mean ± SEM. No data were excluded from the analysis.

Data availability

The original data of this study are available from R.P. upon reasonable request.

Results

Murine embryonic MGE progenitor cells migrate widely following early postnatal transplantation into the recipient mouse brain[18]. Within the host brain, transplanted MGE-derived interneurons efficiently distribute across cortical layers[30–32]. However, residual clustering and limited migration away from the injection site have also been reported[29,33]. Since factors transiently expressed in the developing brain, e.g., clustered gamma-protocadherins[34,35] or CCCTC-binding factor[36], can influence migration and integration of MGE progenitor cells, we investigated here the integration following transplantation into recipient mice at different developmental ages. Because factors expressed in local microcircuits, e.g., vesicular GABA transporters[32] or MTG8[37], can also influence integration of these progenitors, we compared transplantations into the cortex and hippocampus (Fig. 1A).

MGE progenitors transplanted into cortex

To investigate the influence of host brain age on survival, migration, and maturation, we harvested MGE progenitor cells from E13.5 GFP-labeled donor embryos and transplanted into the neocortex of neonatal (P2–P4), juvenile (P30–40), and adult (P60–150) mice. At 30 days post-transplantation (DAT), we noted a significant difference in cell survival across the three age groups, with higher GFP+ cell survival rate following transplantation into neonatal host brains compared to juvenile or adult mice (P2–4, 17.2 ± 2.5%, n = 8 mice; P30–40, 0.8 ± 0.1%, n = 6 mice; P60–150, 0.7 ± 0.1%, n = 5 mice; $p < 0.001$, one-way ANOVA). We also found a significant difference in migration capacity away from the injection site. At 30 days after a single cortical injection of MGE-GFP progenitors in neonates (n = 8), GFP + cells showed extensive distribution along the antero-posterior, medial–lateral, and dorsal–ventral axes (Fig. 1B–E). In the anterior-posterior direction, cells migrated up to 3000 µm from the injection site in both directions, covering the entire antero-posterior cortical structures (up to anterior cingulate and visual cortex in the anterior and posterior axes, respectively). Along the dorsal–ventral axis, in addition to neocortex, MGE-GFP cells reached into striatum, dorsal subiculum and in some cases, CA1 regions of the hippocampus (Fig. 1D). Across the medial–lateral extent of neocortex, MGE-GFP cells reached lateral cortical areas, such as the auditory cortex. In juvenile and adult host brains, although transplanted MGE-GFP progenitor cells migrated away from the injection site, the distance reached in antero-posterior axis was more limited (up to 600 µm) (Fig. 2). The total anterior-posterior cortical distances covered were 3825 ± 239 µm (neonate), 850 ± 92 µm (juvenile), and 900 ± 95 µm (adult) ($p < 0.001$, one-way ANOVA).

Next, to assess the laminar distribution of MGE-derived GFP+ cells within specific cortical sub-layers of the host brain, we divided the radial axis of the cortex into ten equal bins and assigned each GFP+ cell to a single bin (see Methods). In the neonatal (P2–P4) transplantation group, GFP+ cells were distributed across the entire neocortex, from Layer II to VI (Fig. 3), and no cells were identified in Layer I (corresponding to bin 1). This distribution matched the endogenous distribution of MGE-derived interneurons in the cortex[30–32]. In

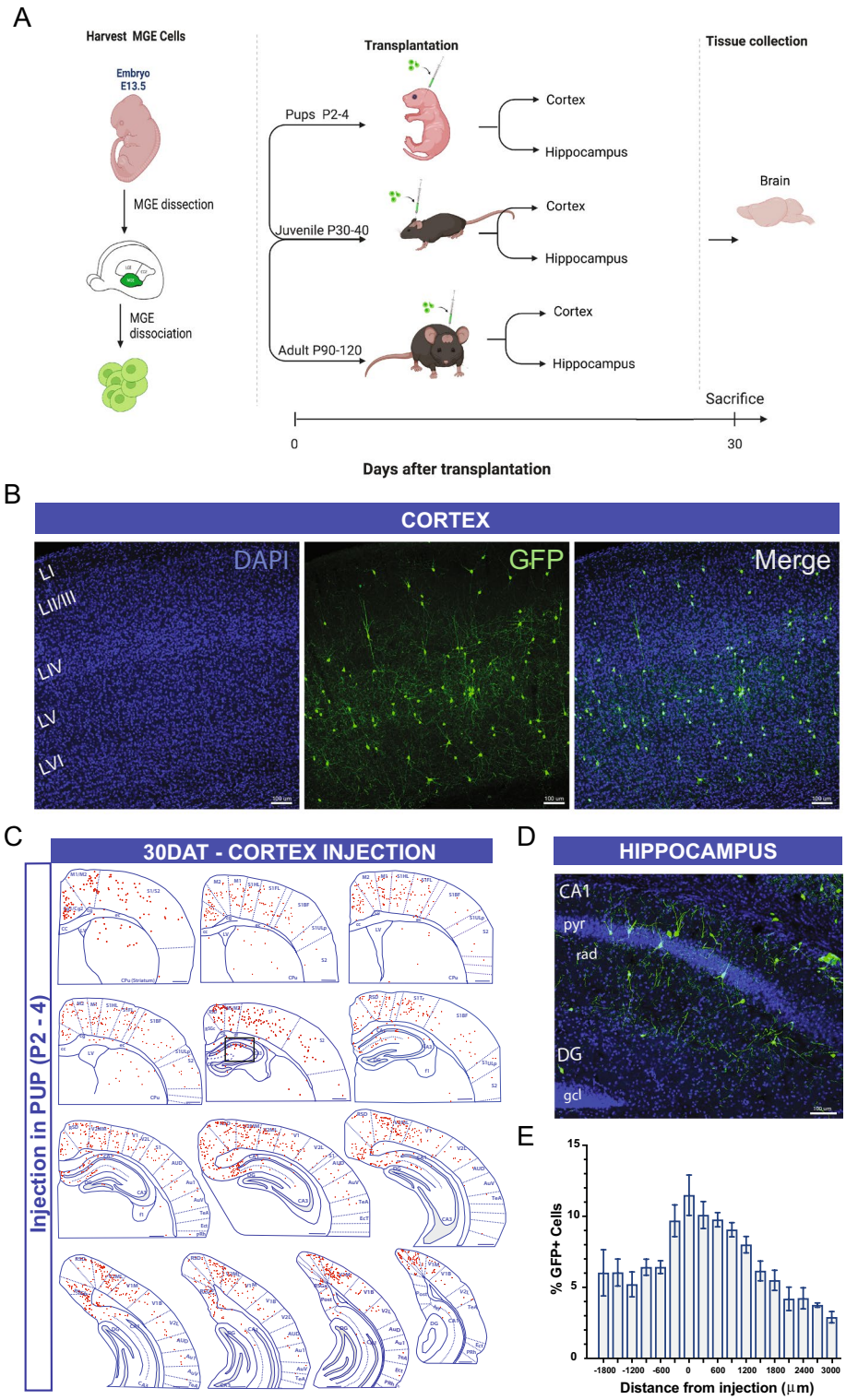

Figure 1. Timeline and distribution of transplanted MGE progenitors in pup cortex. (**A**) schematic of the overall experimental design. (**B**) Coronal section of a pup recipient mouse (30 DAT) labeled for transplanted GFP+ neurons (green). Transplanted cells widely dispersed across the cortex. (**C**) Schematic at 30 DAT showing the distribution of GFP+ cells (red) across brain slices in the antero-posterior axis (300 µm apart) after transplantation in pup cortex. Region divisions were adapted from the Paxinos atlas. (**D**) Higher magnification of the hippocampal region outlined in B. (**E**) Plot showing the distribution of GFP+ cells along the antero-posterior axis 30 DAT cortex injection in pup (P2–4) mice; n = 8 brains. DAT, days after transplantation. Data are represented as mean ± SEM.

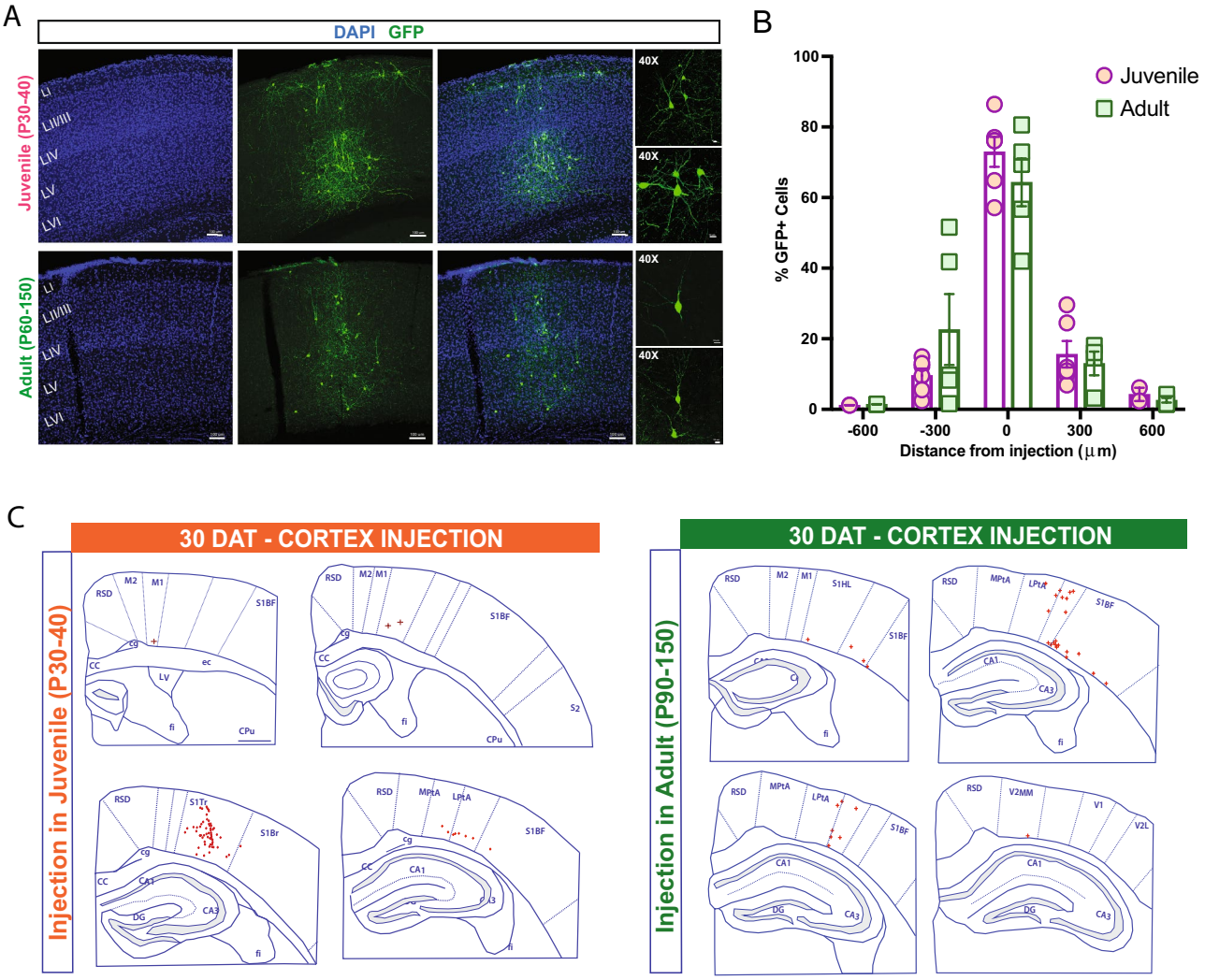

Figure 2. Transplanted MGE progenitors in juvenile and adult cortex. (**A**) Representative images from 30 DAT brains receiving MGE progenitor cells in the cortical area at P30 (juvenile, top) and P90 (adult, bottom). (**B**) Plot showing the distribution of GFP+ cells in the antero-posterior axis from the injection site in juvenile (P30–40) mice; n = 6 brains and adult (P60–150) mice, n = 5 brains. (**C**) Schematic at 30 DAT showing the distribution of GFP+ cells (red) across brain slices in the antero-posterior axis (300 μm apart) after transplantation in juvenile (left panel) and adult (right panel) cortex. Region divisions were adapted from the Paxinos atlas. DAT, days after transplantation. Data are represented as mean ± SEM.

the juvenile (P30–40) and adult (P60-150) transplantation groups, we observed a similar distribution of GFP+ cells across layers. However, an increased number of transplant-derived cells were observed in the deep cortical layers (bin 10) near injection sites in adult compared to pup and juvenile mice (Fig. 3A,B). We also found a significant increase in GFP+ cells along the medial–lateral axis that migrate laterally from the injection site after transplantation in neonatal host brains compared to juveniles and adults (P2–4, 5229 ± 80.1 mm, n = 8 mice; P30–40, 970 ± 66.6 mm, n = 6 mice; P60–150, 994 ± 62 mm, n = 5 mice; $p < 0.001$, one-way ANOVA) (Fig. 3C). Interestingly, in juvenile and adult brains, transplanted-derived cells appeared to have a columnar distribution, while in pup brains, they were broadly distributed.

To evaluate the temporal migration profile after transplantation, we analyzed the cortical grafted GFP+ cells in the adult (P60–150) transplantation groups at 7 and 14 DAT. As previously shown in pup transplantation[18], the antero-posterior migration of the grafted MGE-derived cells is already completed by 7 DAT, with GFP+ cells located up to 600 μm from the injection site. Additionally, we noted that the GFP+ cell survival rate following transplantation was similar to the rate observed at 30 DAT (7 DAT, 2.1 ± 0.7%, n = 5 mice; 14 DAT, 1 ± 0.4%, n = 5 mice; 30 DAT, 0.7 ± 0.1%, n = 5 mice; $p > 0.05$ one-way ANOVA). These findings indicate that the majority of the GFP+ cells in the cortex have reached their final destination at 7 DAT and are already initiating the maturation process.

To evaluate whether the host brain environment influences maturation of MGE-derived GFP+ cells, we performed a series of immunohistochemical studies using antibodies recognizing neurons (NeuN), interneurons (PV and SST), and glia (GFAP, Olig2 and CC1). In the neonatal (P2–P4) transplantation group, GFP+ cells were primarily NeuN-positive and co-labeled with PV or SST, as expected for MGE-lineage interneurons[15,38]. GFP+

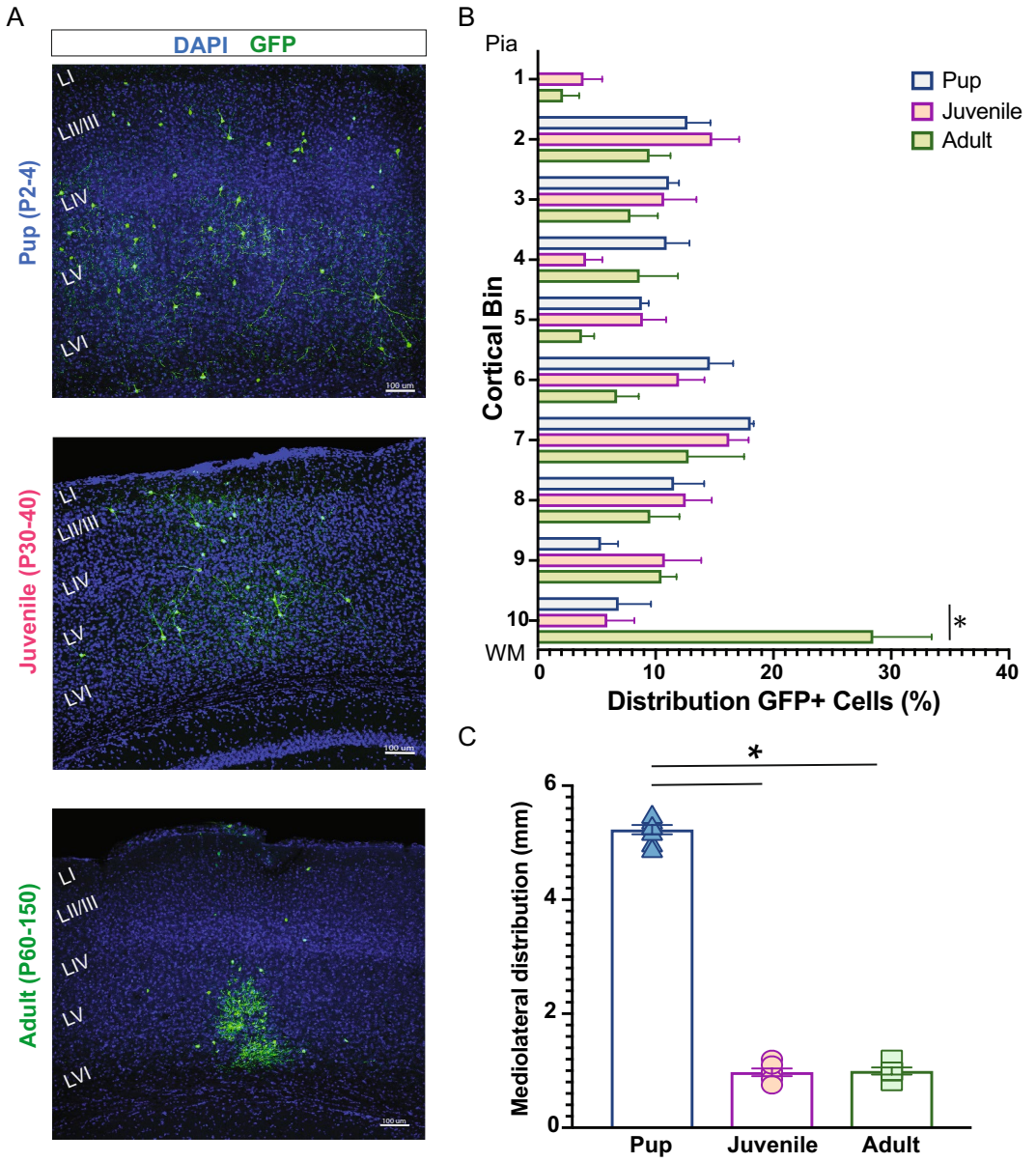

Figure 3. Distribution of MGE-derived cells following transplantation in cortex. (**A**) Representative coronal sections at 30 DAT after pup (top), juvenile (middle), and adult (bottom) transplantation. (**B**) Plot showing the distribution of MGE-derived cells along the rostro-caudal axis divided into 10 bins from pia to white matter (WM). Note comparable distribution across different age groups, except for an increased number of GFP+ cells close to the injection site in adults (bin 10). (**C**) Plot of the mediolateral distribution of cells across age groups. Note a highly mediolateral migration after pup transplantation. DAT, days after transplantation. Data are represented as mean ± SEM; one-way ANOVA $^{*}p < 0.05$.

cells did not co-label with glial markers (Fig. 4A,B). In the juvenile (P30–40) transplantation group, a similar distribution of NeuN+, PV+ and SST+ co-labeled MGE-GFP cells was observed, with few to no GFP+ cells co-labeled with GFAP, Olig2, or CC1, excluding the injection site. In the adult (P60-150) transplantation group, we noted an overall decrease in NeuN+ neurons (Fig. 4B) and specifically PV+ interneurons compared to younger transplantation groups (P2–4, PV: 28 ± 2.3%; P30–40, PV: 16.6 ± 4%; P60–150, PV: 10.5 ± 2%, $p < 0.01$, one-way ANOVA). However, GFP+ cells co-expressed a similar proportion of SST (P2–4, SST: 33 ± 1.8%; P30–40, SST: 34.7 ± 3.4%; P60–150, SST: 30.9 ± 4.2%, $p = 0.7$, one-way ANOVA). Interestingly, in juvenile and adult groups, we observed a few GFP+ cells co-expressing GFAP concentrated at the injection sites, surrounded by an increased number of endogenous GFAP+ cells surrounding the injection site compared to the adjacent cortical area, as shown in Fig. 5A. At distances of 300 um away from the injection site, MGE–GFP cells differentiated into cells with a neuronal morphology, expressing neuron- and interneuron-specific markers (Fig. 5B). Taken together,

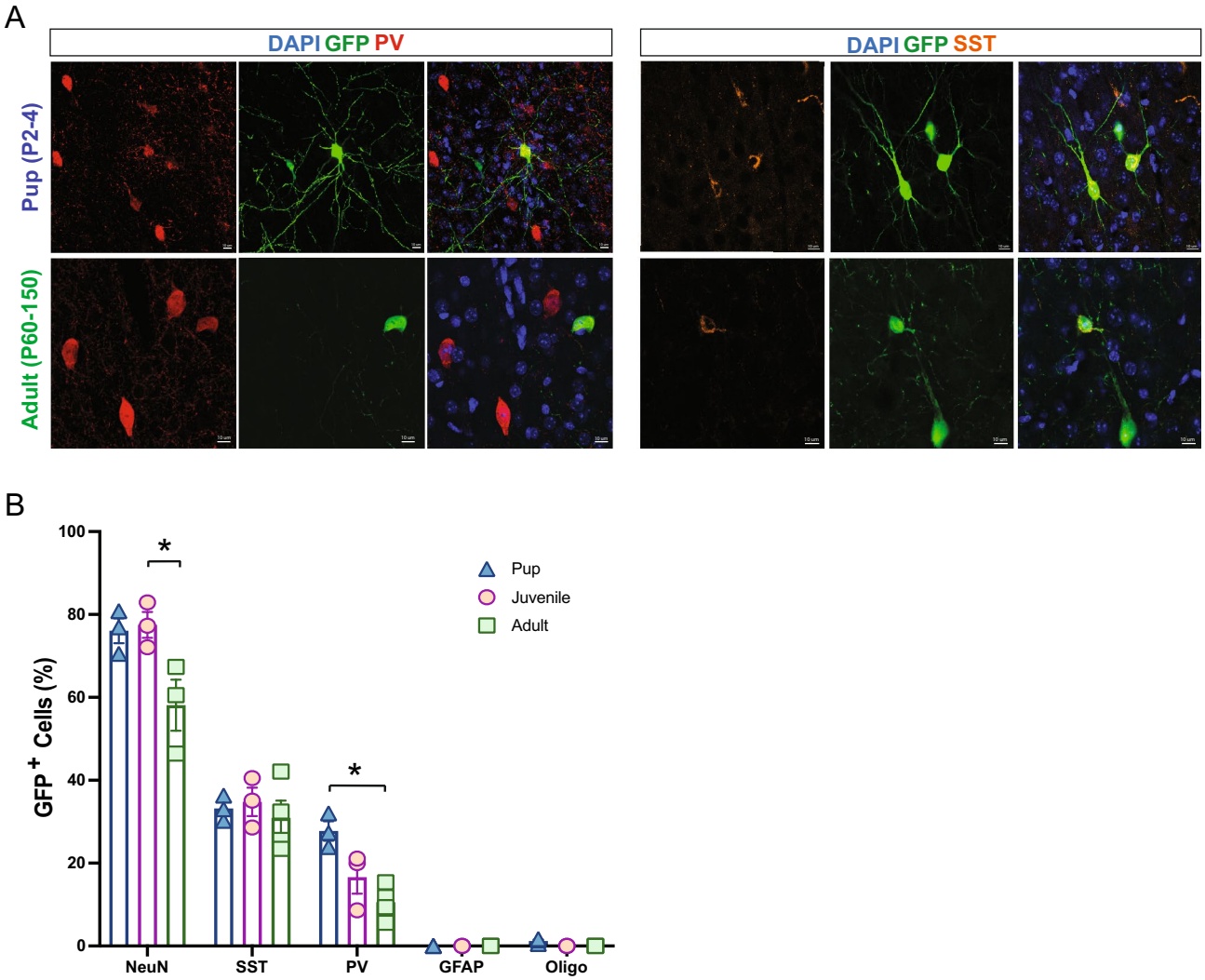

Figure 4. Maturation profile for MGE-derived interneurons transplanted in cortex. (**A**) Representative magnified cell images showing co-localization between GFP and PV (left side) and SST (right side) at 30 DAT after pup and adult transplantation. (**B**) Plot showing the quantification of marker expression in GFP-labeled cells (n = 3 mice per marker) across age groups. Note a decreased number of GFP co-expressing PV cells in juvenile and adult groups. Data are represented as mean ± SEM; one-way ANOVA *$p < 0.05$. DAT, days after transplantation. NeuN, neuronal nuclei; SST, somatostatin; PV, parvalbumin; GFAP, glial fibrillary acid protein; Oligo, oligodendrocyte.

these findings suggest that the neonatal cortex is a more permissible environment for the transplantation of MGE progenitor cells compared to later stages of development.

MGE progenitors transplanted into hippocampus

To investigate whether local host brain microcircuits influence the survival, migration, or maturation of transplanted MGE progenitor cells, we targeted the hippocampus. This complex brain region has a unique anatomical structure and is widely implicated in the pathophysiology of neurological diseases[39]. MGE progenitors from E13.5 GFP-labeled donor embryos were transplanted into the hippocampus of neonatal (P2–P4), juvenile (P30–40), and adult (P60–150) mice. At 30 DAT, we noted a significant difference in cell survival across the three age groups. A higher hippocampal GFP+ cell survival rate was noted in pups compared to juvenile and adult mice (P2–4, 8.7 ± 0.6%, n = 6 mice; P30–40, 0.98 ± 0.2%, n = 6 mice; P60–150, 0.7 ± 0.08%, n = 7 mice; $p < 0.001$, one-way ANOVA). Migration away from the injection site was also different across the three age groups. In particular, after a single injection of MGE progenitor cells in the pup hippocampus, transplanted cells distributed widely across the entire antero-posterior axis of the hippocampus (up to 2400 µm from the injection site), with GFP+ cells spreading into the dorsal and ventral hippocampus, as shown in Fig. 6A–C. In some cases (4 out of 6 mice), a few GFP+ transplanted cells migrated and spread into cortical areas and transition subiculum (Fig. 6B); note that the average GFP+ survival rate outside the hippocampus was 5.9 ± 1.5% (n = 6 mice). Migration in juvenile and adult mice (Fig. 7A) was more limited, reaching up to 900 μm from the injection site (Fig. 7B,C).

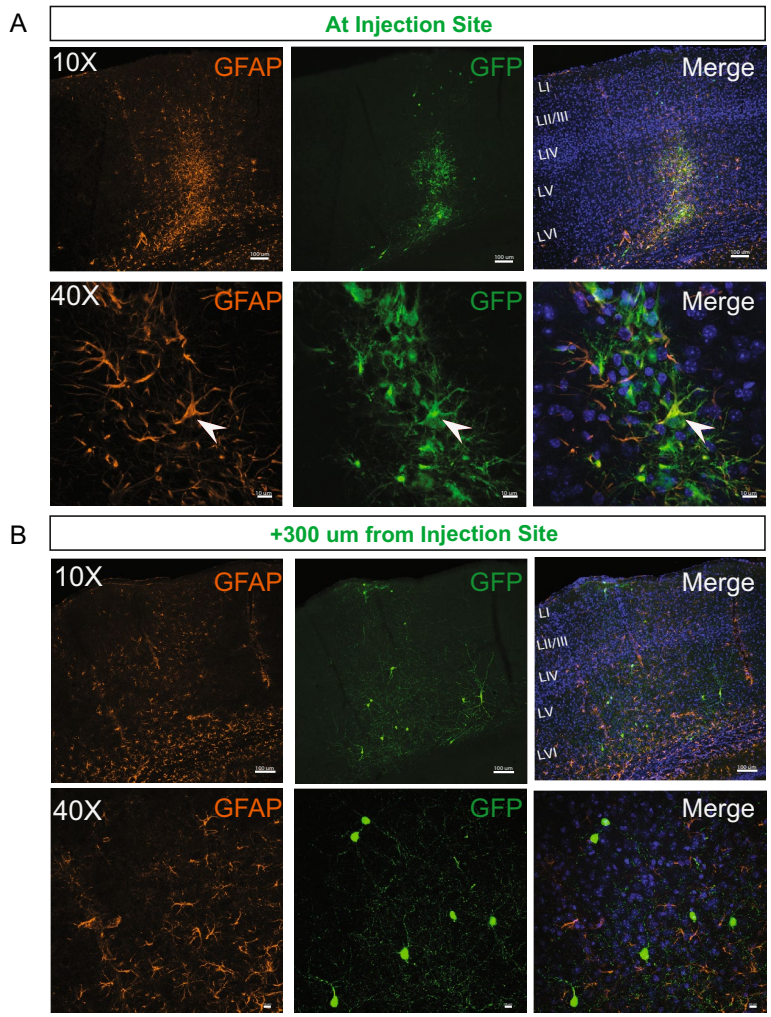

Figure 5. Endogenous astrocyte expression at the injection site. (**A**) Representative images collected at the injection site of an animal at 30 DAT. Note the presence of endogenous astrocytes (GFAP) around the cortical injection site and a few GFP+ astrocytes (white arrow). (**B**) Representative images collected 300 µm away from the injection site from the same animal. GFP+ cells show mature neuronal morphology. DAT, days after transplantation. GFAP, glial fibrillary acid protein.

In all age groups (pup, juvenile, and adult), the transplant-derived cell distribution within the hippocampus was not uniform, and an increased number of GFP+ cells were observed in specific subregions. For example, at 30 DAT in the hippocampal dentate gyrus (DG) of pups, GFP+ cells were primarily found in DG, with only few cells in CA1 and CA3 subregions (74%, 21.4%, and 4.5%, respectively; $p < 0.001$, one-way ANOVA) (Fig. 8A). In adult mice, cells transplanted in area CA3 migrated mostly within the CA3 subregions (70%), with only few cells reaching CA1 or DG (Fig. 8B). In one case, we observed extensive migration of GFP+ cells in DG after injection in CA3 stratum radiatum. These results highlight that, in addition to a host brain age effect, within the hippocampus, targeted subregions also influence the migration of transplanted MGE progenitor cells.

Next, we evaluated whether the hippocampal host brain environment influences differentiation of MGE-derived cells. No differences were observed in GFP + cells co-expressing NeuN (P2–4, NeuN: 49.5 ± 1.6%; P30–40, NeuN: 69.1 ± 1.9%; P60–150, NeuN: 70.3 ± 9.1%, $p > 0.05$, one-way ANOVA), PV (P2–4, PV: 9.2 ± 3.1%; P30–40, PV: 6.1 ± 2.4%; P60–150, PV: 3.4 ± 1.8%, $p > 0.05$, one-way ANOVA), Oligo (P2–4, Oligo: 1.6 ± 0.5%; P30–40, Oligo: 6.4 ± 4%; P60–150, Oligo: 0%, $p > 0.05$, one-way ANOVA) and CC1 (P2–4, CC1: 0.9 ± 0.7%; P30–40, CC1: 0.9 ± 0.9%; P60–150, CC1: 0%, $p > 0.05$, one-way ANOVA) across the three age groups (Fig. 9). However, we observed reduced GFP+ cells co-expressing SST in pups compared to juveniles and adults (P2–4, SST: 10.7 ± 1.7%; P30–40, SST: 38 ± 2.7%; P60–150, SST: 36.2 ± 5.4%, $p < 0.01$, one-way ANOVA, Fig. 9B). Surprisingly, around 13% of transplanted MGE progenitor cells in the pup hippocampus (DG area) co-expressed GFAP at 30 DAT (Fig. 10A) while no GFAP+ cells were observed in juvenile or adult mice. GFP+ co-expressing GFAP cells migrated along the antero-posterior axis up to 1500 µm from the injection site (Fig. 10B) and were only located within DG. These cells exhibit morphology, size, and branch orientation similar to molecular astrocytes, recently described by Karp et al.[40], and were distributed across dentate gyrus layers (ML, GZ, SGZ, hilus) similar to endogenous astrocytes (Fig. 10C).

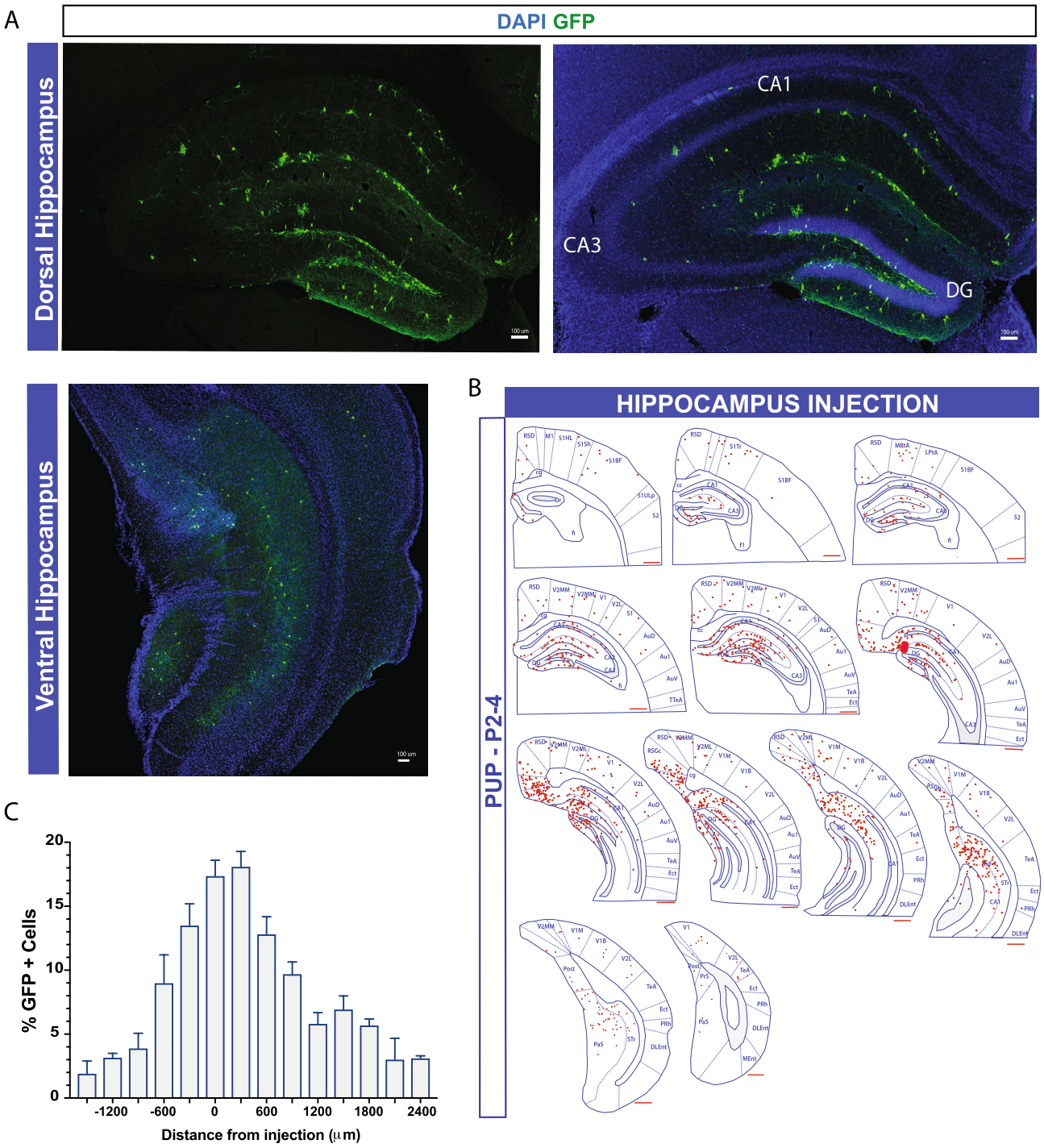

Figure 6. Distribution of MGE-derived cells following transplantation in the hippocampus. (**A**) Representative images of dorsal and ventral hippocampal sections with GFP+ cells. (**B**) Schematic of the distribution of GFP+ cells (marked in red) sectioned 300 μm apart. Region divisions were adapted from the Paxinos atlas. (**B**) Percentage of GFP+ cells across the antero-posterior axis (6 mice, from 3 or more experiments). (**D**) Plot showing the quantification of the total number of GFP+ cells in the hippocampus at 30 DAT of a single injection. DAT, days after transplantation. Data are represented as mean ± SEM.

Discussion

Our results suggest that the host brain environment plays a crucial role in regulating survival, migration, and maturation of cells derived from the transplantation of embryonic MGE progenitors. Although previous work suggested that interneuron survival following transplantation is guided by an intrinsic maturational program rather than the developmental state of the host brain itself[41], our data effectively demonstrate robust survival and extensive migration when MGE progenitors are transplanted early in development (but not later) or into

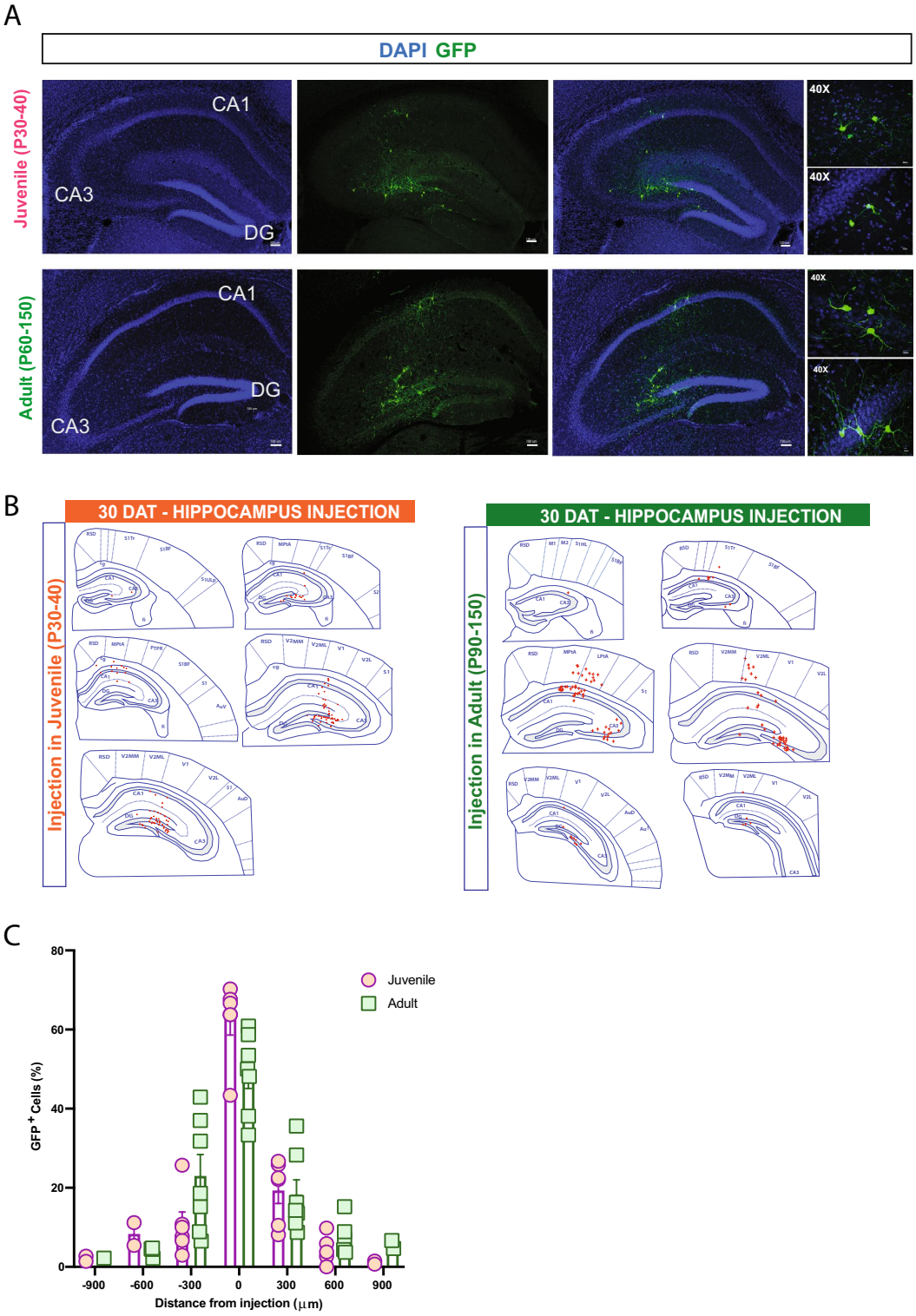

Figure 7. Transplanted MGE progenitors in juvenile and adult hippocampus. (**A**) Representative coronal section of the hippocampus from juvenile (top) and adult (bottom) host brains at 30 DAT showing surviving GFP+ cells (green). Right panels show higher magnification of transplanted cells with interneuronal-like morphology. (**B**) Schematic at 30 DAT showing the distribution of GFP+ cells (red) across brain slices in the antero-posterior axis (300 μm apart) after transplantation in juvenile (left panel) and adult (right panel) hippocampus. Region divisions were adapted from the Paxinos atlas. (**C**) Plot of the percentage of GFP+ cells across the antero-posterior axis (6 mice, from 3 or more experiments). DAT, days after transplantation. Data are represented as mean ± SEM.

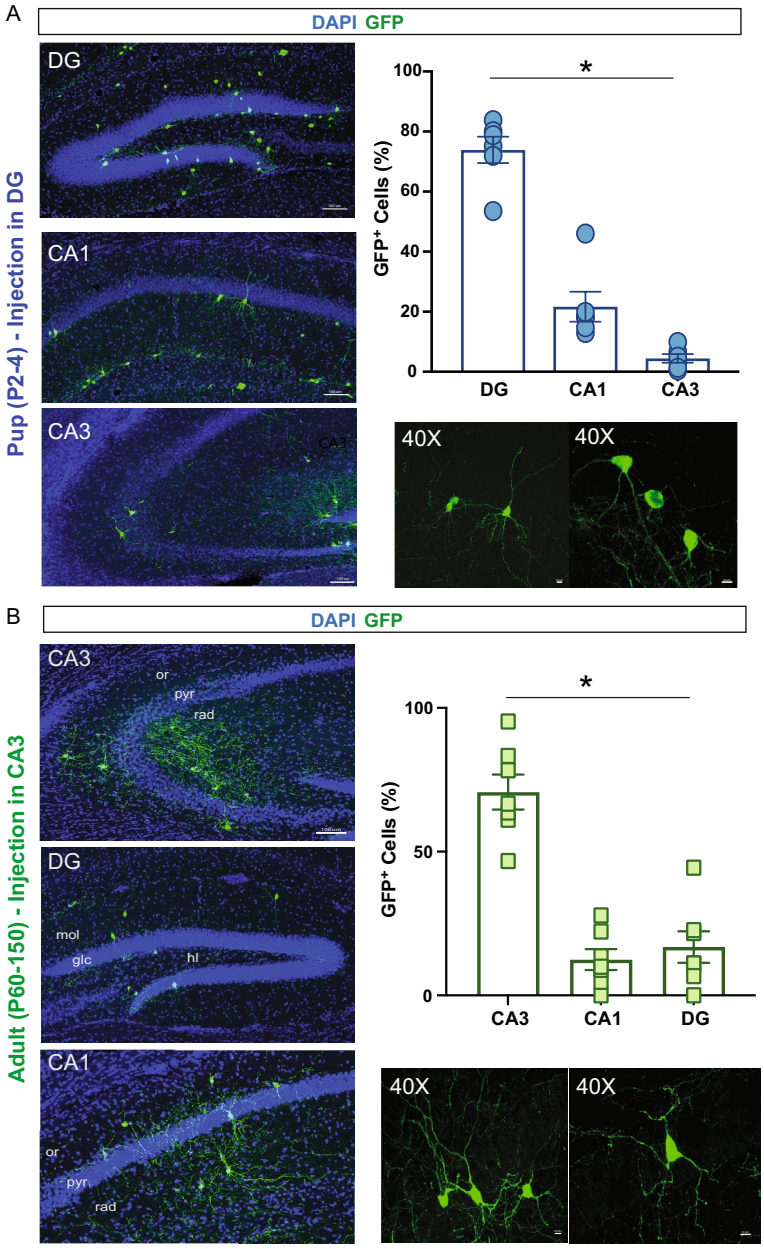

Figure 8. Distribution of transplant-derived MGE–GFP cells within hippocampal subfields. (**A**) Representative hippocampal sections of the subfields CA1, CA3, and DG at 30 DAT after pup injections. Plot showing the quantification of GFP+ cells across the subfields of the hippocampus (6 mice from 3 or more experiments). Note the increased number of cells in the dentate gyrus compare to CA1 and CA3. (**B**) Representative hippocampal sections of the subfields CA1, CA3, and DG at 30 DAT showing the distribution of GFP + cells after adult injections. Quantification of GFP+ cells across the subfields of the hippocampus (6 mice from 3 or more experiments). Note the increased number of cells in CA3 compare to CA1 and DG. Higher resolution examples of GFP+ cells imaged under 40× objective showing a mature neuronal morphology are shown at the bottom. DAT, days after transplantation; GFAP, glial fibrillary acid protein. Data are represented as mean ± SEM; one-way ANOVA $*p < 0.05$.

cortex (compared to hippocampus). The maturation profile of MGE-derived interneurons is also regulated by the developmental state and brain region. We observed a two-fold greater percentage of SST-positive interneurons following hippocampal transplantation into juvenile or adult brains (compared to neonates). In contrast, the percentage of PV-positive interneurons decreased nearly two-fold with age following cortical transplantation into the adult brain compared to neonates. Unexpectedly, we also found sub-regions of pup hippocampus—namely the dentate gyrus—where transplant-derived MGE progenitors locally differentiate into astrocytes. Considering the emerging therapeutic potential of transplanted embryonic MGE progenitors in various neurological disorders[10,11,13,21,25,42], these results hold important clinical implications.

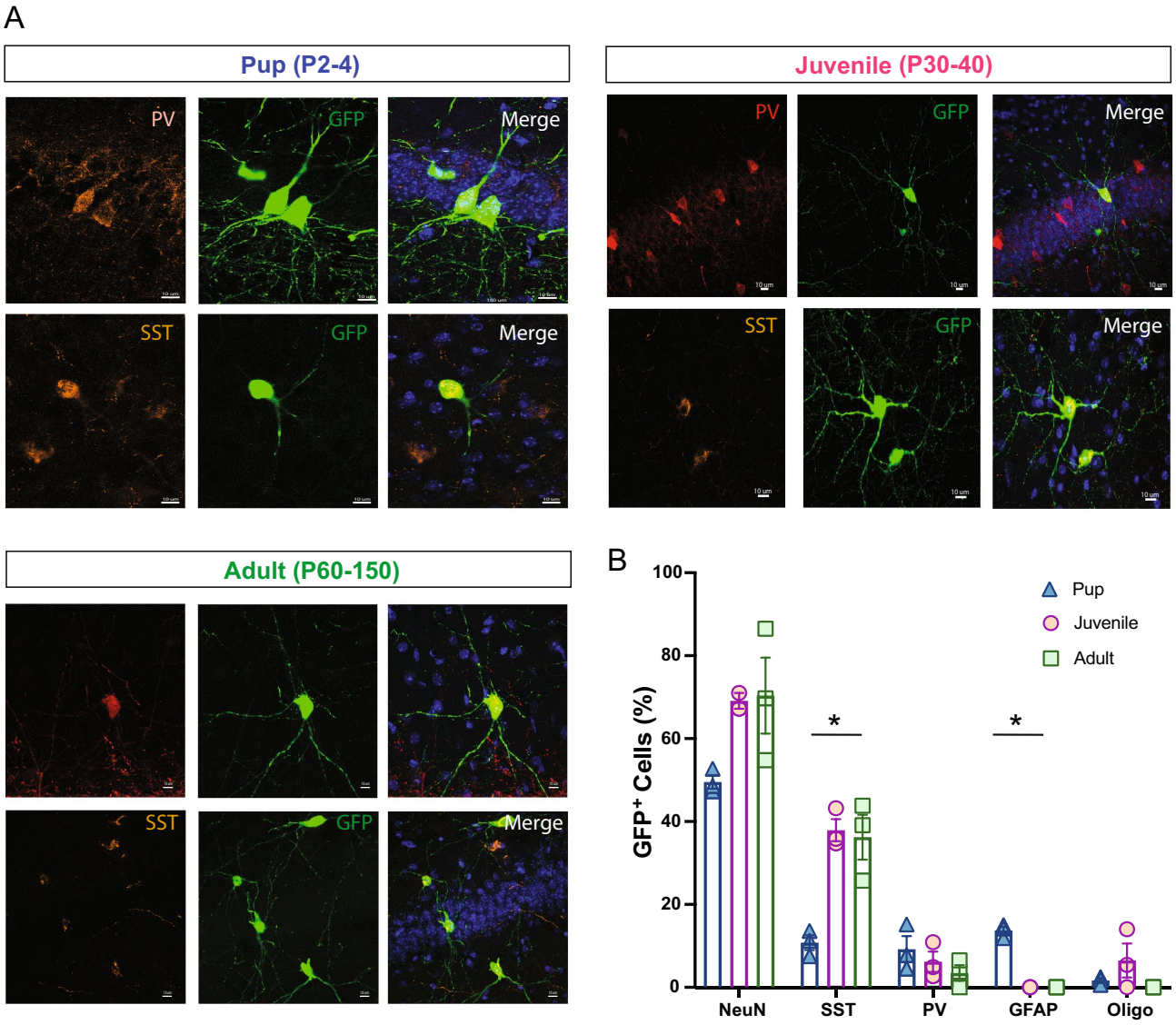

Figure 9. Maturation profile for MGE-derived interneurons transplanted in hippocampus. (**A**) Representative magnified cell images showing GFP+ cells co-expressing PV and SST at 30 DAT in pup, juvenile, and adult hippocampus. (**B**) Plot showing the quantification of cells co-expressing GFP and NeuN, SST, PV, GFAP, and Oligo in the hippocampus at 30 DAT for pup, juvenile, and adult groups (n = 3–4 mice per marker). Note the reduced GFP+ cells co-expressing SST and increased GFP+ co-expressing GFAP cells in the pup group. DAT, days after transplantation. Data are represented as mean ± SEM; one-way ANOVA $*p < 0.05$. Abbreviations as in Fig. 4.

There are several mechanisms that could regulate survival, spatial distribution, and maturation of MGE-derived interneuron subtypes following transplantation. First, activity-dependent mechanisms such as excitatory pyramidal cell activity may serve as critical regulator of interneuron development, establishing age- and region-specific permissive corridors for MGE progenitors[43–45]. In murine neocortex, for instance, spontaneous patterns of activity present at birth[46–48] could facilitate the widespread anterior-to-posterior migration of transplanted MGE progenitors, as observed in our study (Fig. 1). Second, precursors for MGE-derived interneuron subtypes could be subject to programmed cell death during neurodevelopment. This process is regulated by region-specific expression of environmental factors such as *pcdh*[34,35,49], *c-Maf*[50], or *PTEN*[44], which facilitate postnatal survival and/or maturation of PV+ and SST+ interneurons. Given that these expression patterns are developmentally regulated, it is not surprising that juvenile and adult brains were less receptive to the integration of transplanted MGE progenitors than mouse pups or the differences in PV/SST ratios seen here (Fig. 4).

In our study, only few GFP+ cells co-expressed classical oligodendrocyte[51–53] or astrocyte[54] markers around the injection site following MGE transplantation in juvenile/adults mice, as previously reported[10,18,33,55]. Surprisingly, following MGE transplantation into the pups' hippocampus, a significant population of GFP+ cells co-expressing GFAP was distributed around the DG layers showing an endogenous astrocyte-like morphology. Numerous studies have shown that glia cells can also originate from Nkx2.1-expressing precursor of embryonic MGE[56]. After

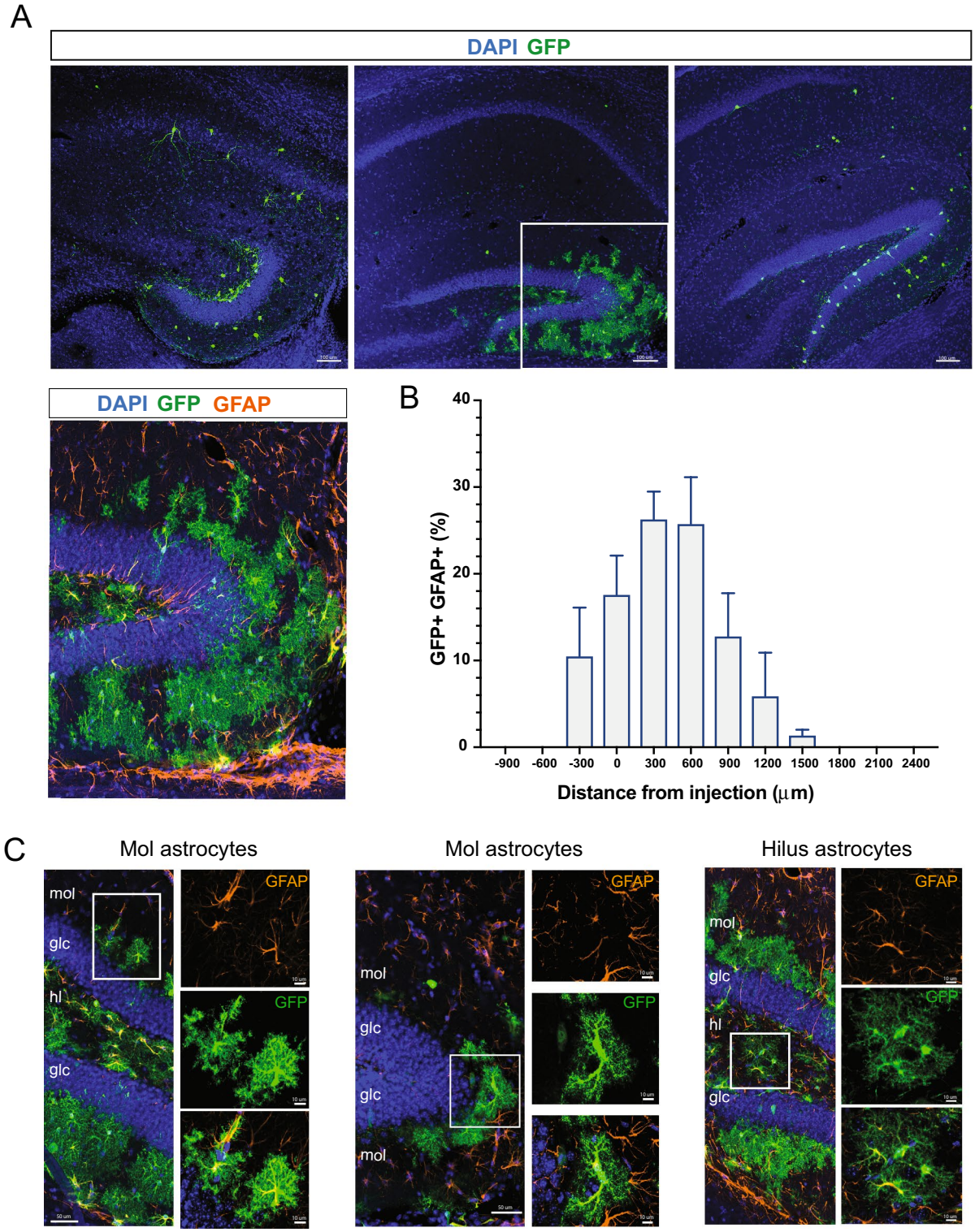

Figure 10. Morphologically distinct astrocytes across DG layers. (**A**) Representative coronal images of GFP+ cells in the hippocampus at different antero-posterior levels following transplantation at P2–4. Higher resolution image of the dentate gyrus showing the distribution of GFP+ co-expressing GFAP across dentate gyrus layers (bottom, left). (**B**) Plot showing the distribution of GFP+ co-expressing GFAP across the antero-posterior axis. (**C**) Representative images of GFP+ co-expressing GFAP cell morphologies at the molecular layer (left, middle) and hilus (right). Higher magnification (40× objective; white box) images of cells are shown at right. DAT, days after transplantation. Data are represented as mean ± SEM.

migrating into the cortex, they transiently participate in cortical neurodevelopment before being replaced by other glia cell populations[57]. Furthermore, earlier studies showed the absence of proliferative markers following transplantation of embryonic MGE progenitors[22,58]. While unlikely, the presence of proliferating neural cells cannot be fully excluded. Future studies focused on additional markers and lineage analysis will be necessary to identify factor(s) driving astrocyte survival following transplantation into the DG microenvironment.

In our hands, MGE transplantation at postnatal day 2 consistently resulted in widespread migration, in all directions, within the host brain parenchyma[18,26,30]. The transplanted MGE progenitor cells also show clear morphologies consistent with migrating cells[18]. Our results confirm and extend these reports. While the possibility that some MGE-GFP cells reached distant sites via the meninges or leakage into the cerebral spinal fluid cannot be entirely excluded due to the small size of the mouse brain[59], the migratory profiles and properties of MGE-derived cells both in vivo and in vitro do not support this conclusion. However, it is interesting that in wild-type juvenile or adult mice, the migratory ability is more limited. The differences in molecular, cellular, and extracellular profiles in the adult versus pup environments[60,61] may explain this reduced migration in the mature brain compared to early developmental stages. Such difference, rather than being a limitation of the technique, highlights the translational applicability of this approach. The ability to modify host circuits with regional and neuronal specificity in the mature brain contrasts with the broad, non-specific circuit changes observed after pups' transplantation. Indeed, adult MGE transplantation has already proven to be an effective disease-modifying therapy in adult mouse models representing acquired epilepsy or traumatic brain injury[10,12,23].

It is worth noting that a significant proportion of individuals with epilepsy, autism spectrum disorders, or schizophrenia are considered to have "inter-neuropathies", define by frank reductions or dysfunction in PV+ and/or SST+ interneurons[3,62–64]. Given that these conditions manifest at different stages of development and that interneuron deficits can be localized to specific cortical or hippocampal brain regions, a better understanding of the influence of local environment on transplanted MGE progenitors is necessary. Indeed, several studies using embryonic MGE progenitors[65] or other embryonic cell sources[66,67] for transplantation also support our findings, emphasizing the significant impact of local environmental factors on the integration of these cells in the host brain. Understanding advantages and limitations of where (and when) MGE progenitors integrate following transplantation is critical for establishing effective and targeted cell therapies for patients suffering from various neurological disorders.

Received: 6 July 2023; Accepted: 19 January 2024
Published online: 13 February 2024

References

1. Sohal, V. S. & Rubenstein, J. L. R. Excitation-inhibition balance as a framework for investigating mechanisms in neuropsychiatric disorders. *Mol. Psychiatry* **24**, 1248–1257 (2019).
2. Dienel, S. J. & Lewis, D. A. Alterations in cortical interneurons and cognitive function in schizophrenia. *Neurobiol. Dis.* **131**, 104208 (2019).
3. Paterno, R., Casalia, M. & Baraban, S. C. Interneuron deficits in neurodevelopmental disorders: Implications for disease pathology and interneuron-based therapies. *Eur. J. Paediatr. Neurol.* **24**, 81–88 (2020).
4. Xu, Y., Zhao, M., Han, Y. & Zhang, H. GABAergic inhibitory interneuron deficits in Alzheimer's disease: Implications for treatment. *Front. Neurosci.* **14**, 660 (2020).
5. Marafiga, J. R., Pasquetti, M. V. & Calcagnotto, M. E. GABAergic interneurons in epilepsy: More than a simple change in inhibition. *Epilepsy Behav.* **121**, 106935 (2021).
6. Kato, M. & Dobyns, W. B. X-linked lissencephaly with abnormal genitalia as a tangential migration disorder causing intractable epilepsy: Proposal for a new term, "interneuronopathy". *J. Child Neurol.* **20**, 392–397 (2005).
7. Thomas, G. P. & Jobst, B. C. Critical review of the responsive neurostimulator system for epilepsy. *Med. Dev. Evid. Res.* **8**, 405-411 (2015).
8. Chiken, S. & Nambu, A. Mechanism of deep brain stimulation: Inhibition, excitation, or disruption?. *The Neurosci.* **22**, 313–322 (2016).
9. Hunt, R. F. & Baraban, S. C. Interneuron transplantation as a treatment for epilepsy. *Cold Spring Harb. Perspect. Med.* **5**, (2015).
10. Hunt, R. F., Girskis, K. M., Rubenstein, J. L., Alvarez-Buylla, A. & Baraban, S. C. GABA progenitors grafted into the adult epileptic brain control seizures and abnormal behavior. *Nat. Neurosci.* **16**, 692–697 (2013).
11. Martinez-Losa, M. *et al.* Nav1.1-overexpressing interneuron transplants restore brain rhythms and cognition in a mouse model of Alzheimer's disease. *Neuron* **98**, 75-89 (2018).
12. Zhu, B., Eom, J. & Hunt, R. F. Transplanted interneurons improve memory precision after traumatic brain injury. *Nat. Commun.* **10**, 5156 (2019).
13. Tong, L. M. *et al.* Inhibitory interneuron progenitor transplantation restores normal learning and memory in ApoE4 knock-in mice without or with Aβ accumulation. *J. Neurosci.* **34**, 9506–9515 (2014).
14. Wichterle, H., Garcia-Verdugo, J. M., Herrera, D. G. & Alvarez-Buylla, A. Young neurons from medial ganglionic eminence disperse in adult and embryonic brain. *Nat. Neurosci.* **2**, 461–466 (1999).
15. Xu, Q., Cobos, I., De La Cruz, E., Rubenstein, J. L. & Anderson, S. A. Origins of cortical interneuron subtypes. *J. Neurosci.* **24**, 2612–2622 (2004).
16. Lim, L., Mi, D., Llorca, A. & Marín, O. Development and functional diversification of cortical interneurons. *Neuron* **100**, 294–313 (2018).
17. Williams, R. H. & Riedemann, T. Development, diversity, and death of MGE-derived cortical interneurons. *Int. J. Mol. Sci.* **22**, 9297 (2021).
18. Alvarez-Dolado, M. *et al.*. Cortical inhibition modified by embryonic neural precursors grafted into the postnatal brain. *J. Neurosci.* **26**, 7380–7389 (2006).
19. Howard, M. A. & Baraban, S. C. Synaptic integration of transplanted interneuron progenitor cells into native cortical networks. *J. Neurophysiol.* **116**, 472–478 (2016).
20. Hsieh, J.-Y. & Baraban, S. C. Medial ganglionic eminence progenitors transplanted into hippocampus integrate in a functional and subtype-appropriate manner. *eneuro* **4** (2017).
21. Baraban, S. C. *et al.*. Reduction of seizures by transplantation of cortical GABAergic interneuron precursors into Kv1.1 mutant mice. *Proc. Natl. Acad. Sci.* **106**, 15472–15477 (2009).

22. Martínez-Cerdeño, V. *et al.* Embryonic MGE precursor cells grafted into adult rat striatum integrate and ameliorate motor symptoms in 6-OHDA-lesioned rats. *Cell Stem Cell* **6**, 238–250 (2010).
23. Casalia, M. L., Howard, M. A. & Baraban, S. C. Persistent seizure control in epileptic mice transplanted with gamma-aminobutyric acid progenitors. *Ann. Neurol.* **82**, 530–542 (2017).
24. Bráz, J. M., Wang, X., Guan, Z. & Basbaum, A. I. Transplant-mediated enhancement of spinal cord GABAergic inhibition reverses paclitaxel-induced mechanical and heat hypersensitivity. *Pain* **156**, 1084–1091 (2015).
25. Perez, S. M. & Lodge, D. J. Hippocampal interneuron transplants reverse aberrant dopamine system function and behavior in a rodent model of schizophrenia. *Mol. Psychiatry* **18**, 1193–1198 (2013).
26. Southwell, D. G. *et al.* Interneuron transplantation rescues social behavior deficits without restoring wild-type physiology in a mouse model of autism with excessive synaptic inhibition. *J. Neurosci.* **40**, 2215–2227 (2020).
27. Tanaka, D. H., Toriumi, K., Kubo, K., Nabeshima, T. & Nakajima, K. GABAergic precursor transplantation into the prefrontal cortex prevents phencyclidine-induced cognitive deficits. *J. Neurosci.* **31**, 14116–14125 (2011).
28. Rosell-Valle, C. *et al.*. GABAergic deficits in absence of LPA1 receptor, associated anxiety-like and coping behaviors, and amelioration by interneuron precursor transplants into the dorsal hippocampus. *Brain Struct. Funct.* **226**, 1479–1495 (2021).
29. Jaiswal, M. K. *et al.*. Reduction in focal ictal activity following transplantation of MGE interneurons requires expression of the $GABA_A$ receptor α4 subunit. *Front. Cell Neurosci.* **9**, 127 (2015).
30. Sebe, J. Y., Looke-Stewart, E., Dinday, M. T., Alvarez-Buylla, A. & Baraban, S. C. Neocortical integration of transplanted GABA progenitor cells from wild type and GABAB receptor knockout mouse donors. *Neurosci. Lett.* **561**, 52–57 (2014).
31. Davis, M. F. *et al.*. Inhibitory neuron transplantation into adult visual cortex creates a new critical period that rescues impaired vision. *Neuron* **86**, 1055–1066 (2015).
32. Priya, R. *et al.* Vesicular GABA transporter is necessary for transplant-induced critical period plasticity in mouse visual cortex. *J. Neurosci.* **39**, 2635–2648 (2019).
33. Daadi, M. M. *et al.*. Functional engraftment of the medial ganglionic eminence cells in experimental stroke model. *Cell Transplant.* **18**, 815–826 (2009).
34. Mancia Leon, W. R. *et al.* Clustered gamma-protocadherins regulate cortical interneuron programmed cell death. *eLife* **9**, e55374 (2020).
35. Pancho, A. *et al.*. Modifying PCDH19 levels affects cortical interneuron migration. *Front. Neurosci.* **16**, 887478 (2022).
36. Elbert, A. *et al.* CTCF governs the identity and migration of MGE-derived cortical interneurons. *J. Neurosci.* **39**, 177–192 (2019).
37. Asgarian, Z. *et al.* MTG8 interacts with LHX6 to specify cortical interneuron subtype identity. *Nat. Commun.* **13**, 5217 (2022).
38. Lavdas, A. A., Grigoriou, M., Pachnis, V. & Parnavelas, J. G. The medial ganglionic eminence gives rise to a population of early neurons in the developing cerebral cortex. *J. Neurosci.* **19**, 7881–7888 (1999).
39. Small, S. A., Schobel, S. A., Buxton, R. B., Witter, M. P. & Barnes, C. A. A pathophysiological framework of hippocampal dysfunction in ageing and disease. *Nat. Rev. Neurosci.* **12**, 585–601 (2011).
40. Karpf, J. *et al.* Dentate gyrus astrocytes exhibit layer-specific molecular, morphological and physiological features. *Nat. Neurosci.* **25**, 1626–1638 (2022).
41. Southwell, D. G. *et al.* Intrinsically determined cell death of developing cortical interneurons. *Nature* **491**, 109–113 (2012).
42. Gilani, A. I. *et al.* Interneuron precursor transplants in adult hippocampus reverse psychosis-relevant features in a mouse model of hippocampal disinhibition. *Proc. Natl. Acad. Sci.* **111**, 7450–7455 (2014).
43. Blanquie, O. *et al.*. Electrical activity controls area-specific expression of neuronal apoptosis in the mouse developing cerebral cortex. *eLife* **6**, e27696 (2017).
44. Wong, F. K. *et al.*. Pyramidal cell regulation of interneuron survival sculpts cortical networks. *Nature* **557**, 668–673 (2018).
45. Wong, F. K. *et al.*. Serotonergic regulation of bipolar cell survival in the developing cerebral cortex. *Cell Rep.* **40**, 111037 (2022).
46. Picken Bahrey, H. L. & Moody, W. J. Early development of voltage-gated ion currents and firing properties in neurons of the mouse cerebral cortex. *J. Neurophysiol.* **89**, 1761–1773 (2003).
47. Tezuka, Y., Hagihara, K. M., Ohki, K., Hirano, T. & Tagawa, Y. Developmental stage-specific spontaneous activity contributes to callosal axon projections. *eLife* **11**, e72435 (2022).
48. Suárez, R. *et al.* Cortical activity emerges in region-specific patterns during early brain development. *Proc. Natl. Acad. Sci.* **120**, e2208654120 (2023).
49. Carriere, C. H. *et al.* The γ-protocadherins regulate the survival of GABAergic interneurons during developmental cell death. *J. Neurosci.* **40**, 8652–8668 (2020).
50. Pai, E. L.-L. *et al.*. Mafb and c-Maf have prenatal compensatory and postnatal antagonistic roles in cortical interneuron fate and function. *Cell Rep.* **26**, 1157-1173.e5 (2019).
51. Wang, H. *et al.* Region-specific distribution of Olig2-expressing astrocytes in adult mouse brain and spinal cord. *Mol. Brain* **14**, 36 (2021).
52. Valério-Gomes, B., Guimarães, D. M., Szczupak, D. & Lent, R. The absolute number of oligodendrocytes in the adult mouse brain. *Front. Neuroanat.* **12**, 90 (2018).
53. Huang, H., He, W., Tang, T. & Qiu, M. Immunological markers for central nervous system glia. *Neurosci. Bull.* **39**, 379–392 (2023).
54. Yang, Z. & Wang, K. K. W. Glial fibrillary acidic protein: from intermediate filament assembly and gliosis to neurobiomarker. *Trends Neurosci.* **38**, 364–374 (2015).
55. Hammad, M. *et al.* Transplantation of GABAergic interneurons into the neonatal primary visual cortex reduces absence seizures in stargazer mice. *Cereb. Cortex* **25**, 2970–2979 (2015).
56. Kriegstein, A. & Alvarez-Buylla, A. The glial nature of embryonic and adult neural stem cells. *Annu. Rev. Neurosci.* **32**, 149–184 (2009).
57. Kessaris, N. *et al.* Competing waves of oligodendrocytes in the forebrain and postnatal elimination of an embryonic lineage. *Nat. Neurosci.* **9**, 173–179 (2006).
58. Arshad, M. N., Oppenheimer, S., Jeong, J., Buyukdemirtas, B. & Naegele, J. R. Hippocampal transplants of fetal GABAergic progenitors regulate adult neurogenesis in mice with temporal lobe epilepsy. *Neurobiol. Dis.* **174**, 105879 (2022).
59. Bifari, F. *et al.*. Neurogenic radial glia-like cells in meninges migrate and differentiate into functionally integrated neurons in the neonatal cortex. *Cell Stem Cell* **20**, 360-373 (2017).
60. Bathina, S. & Das, U. N. Brain-derived neurotrophic factor and its clinical implications. *Arch. Med. Sci.* **6**, 1164–1178 (2015).
61. Luhmann, H. J. *et al.* Spontaneous neuronal activity in developing neocortical networks: From single cells to large-scale interactions. *Front. Neural Circuits* **10**, 40 (2016).
62. Marín, O. Interneuron dysfunction in psychiatric disorders. *Nat. Rev. Neurosci.* **13**, 107–120 (2012).
63. Katsarou, A., Moshé, S. L. & Galanopoulou, A. S. Interneuronopathies and their role in early life epilepsies and neurodevelopmental disorders. *Epilepsia Open* **2**, 284–306 (2017).
64. Nomura, T. Interneuron dysfunction and inhibitory deficits in autism and fragile X syndrome. *Cells* **10**, 2610 (2021).
65. Quattrocolo, G., Fishell, G. & Petros, T. J. Heterotopic transplantations reveal environmental influences on interneuron diversity and maturation. *Cell Rep.* **21**, 721–731 (2017).
66. Grade, S. *et al.* Brain injury environment critically influences the connectivity of transplanted neurons. *Sci. Adv.* **8**, eabg9445 (2022).
67. Thomas, J. *et al.* Excessive local host-graft connectivity in aging and amyloid-loaded brain. *Sci. Adv.* **8**, eabg9287 (2022).

Acknowledgements
This work was supported by NIH/NINDS grant R01NS-071785-14 to S.C.B. Figure 1A was created with BioRender.com

Author contributions
R.P. and S.C.B. designed research; R.P., T.V. C.H. conducted the research; R.P. and T.V. analyzed data; R.P. and S.C.B. wrote the paper.

Competing interests
The authors declare no competing interests.

Additional information
Correspondence and requests for materials should be addressed to R.P.

Reprints and permissions information is available at www.nature.com/reprints.

Publisher's note Springer Nature remains neutral with regard to jurisdictional claims in published maps and institutional affiliations.